**SWIFT-UVOT-CALDB-##**
Date Original Submitted:
Prepared by: Wayne Landsman
Date Revised:
Revision #02
Revised by:
Pages Changed:
Comments:

# SWIFT UVOT CALDB RELEASE NOTE

SWIFT-UVOT-CALDB-##: LARGE SCALE SENSITIVITY

## 0. Summary:

This product maps the large scale sensitivity variations for the *u*, *b*, and *v* filters of the UVOT.

## 1. Component Files:

| FILE NAME | VALID DATE | RELEASE DATE | VERSION |
|---|---|---|---|
| | | | |
| | | | |
| | | | |

## 2. Scope of Document:

This document contains a description of the Large Scale Sensitivity (LSS) calibration analysis performed to produce the LSS calibration products for the *u*, *b*, and *v* filters in the UVOT calibration database.

## 3. Changes:

This is the first version to discuss large scale sensitivity changes. The large scale variations discussed in the previous version were due to scattered light.

## 4. Reason For Update:

Large scale variations of up to 9% are present in the UVOT photometry that can be corrected with a Large Scale Sensitivity file.

## 5. Expected Updates:

Analysis of the LSS for the UVW1, UVW2 and UVM2 and white filters still needs to be completed.

It may be possible to define the LSS at a finer spatial scale than the bi-quadratic form used here.

## 6. Caveat Emptor:

The LSS correction must be performed ***after*** the coincidence loss correction. It is not a property of the detector and differs for each filter.

Co-added images combine data taken at different raw positions on the detector (due to spacecraft drift and roll). Thus there is no unique LSS factor that can be assigned to a pixel in a co-added image.

The LSS is modelled using a bi-quadratic polynomial in the raw X,Y position. Variations on a higher frequency scale will not be corrected.

## 7. Data Used:

The data to derive the LSS for the *v* filter consists of 68 images of the GD50 field obtained between Dec 2005 and Oct 2006. All exposure times were longer than 100s. Most of these images were obtained in a dithered pattern for the express purpose of determining the LSS. The nominal dither pattern was a 5 by 5 grid with pointings shifted by 3' in both RA and Dec. However, many of the images taken in Dec 2005 are of limited use, because the dither pattern in RA was inadvertently set to 3 minutes of time, rather than 3'. Due to the dither pattern and changing roll angle, not all stars are observed on all images. The white dwarf GD

50 was the star with the largest number of useable pointings (41).

The data to derive the LSS for the *b* filter consists of 140 images of the 3C 279 field obtained during a science monitoring program between Jan 2006 and July 2007. This total include 54 binned images. There was no dithering of these images, but the change in the roll angle during the 18 months of observations allowed stars to appear on different positions on the detector.

The data to derive the *u* filter LSS consists of *u* images obtained during the same 3C 279 monitoring program.

## 8. Description of Analysis:

### A. Overview

The sensitivity variation is modelled as a 2-d quadratic with five free parameters

$$(1): lss = 1 + c_1 * x + c_2 * x^2 + c_3 * x * y + c_4 * y + c_5 * y^2$$

where x and y are measured in raw coordinates from the centre (1024,1024) of the unbinned raw image. The above formula ensures that the LSS correction is unity at the center of the raw image. The coincidence-corrected count rate at a raw X, Y position must be *divided* by the LSS to yield the count rate that would be observed at the center of the detector.

The onboard “shift and add” algorithm will move counts to nearby pixels to account for spacecraft drift during an observation. Thus in image mode the raw pixel location is not precisely defined, but may have a small uncertainty (e.g. 10 pixels for a 5" drift).

In principle, the LSS for each filter could be completely characterized by storing the 5 polynomial coefficients. Currently, however, the LSS is stored as a 2048 by 2048 array giving the sensitivity variation across the raw image. This allows flexibility in case there are future improvements which allow the LSS to be specified on a finer spatial scale.

To derive the coefficients, I use repeated observations of the same field where the position of a star on the detector varies either because of explicit dithering (for the *v* observations of GD 50) or because the roll angle changes (for the *b* and *u* observations of 3C 279). I then use least-squares minimization techniques to adjust the parameters in Eq. (1) to minimize the variance in the stellar photometry. Table 1 lists the number of images and the numbers of stars used for each filter. Each star was weighted by the number of times it was observed . No direct use was made of the photometric errors, but each observation was required to have a minimum signal to noise of 35. In addition, stars located near the haloes of bright saturated stars were not used.

Table 1: Target Fields

| *Filter* | *Field Name* | *# of Inages* | *# of Stars* | *Min* | *Max* |
|---|---|---|---|---|---|
| *v* | GD 50 | 68 | 70 | 0.984 | 1.088 |
| *b* | 3C 279 | 140 | 35 | 0.997 | 1.060 |
| *u* | 3C 279 | 121 | 18 | 0.988 | 1.090 |

It is important that variable stars are not used during the least-squares fitting. This is especially critical for the 3C 279 field because the roll angle changes over a time scale of months, and any variability over this time scale could be mistaken for an LSS effect. The candidate variable stars were manually identified as those showing variability larger than the photometric errors despite minimal changes in the detector position. (The blazar 3C 279 itself is highly variable and cannot be used in the least-squares fitting.) Figure 1 shows the orientation of the 121 raw images obtained during the *u* filter observations of 3C 279. Each edge of the raw image is given a different color so as to make visible the changes in orientation.

B. Results:

Table 2 gives the derived polynomial coefficients for the *v*, *b*, and *u* filters.

Table 2: Derived LSS coefficients

| *Filter* | *C1* | *C2* | *C3* | *C4* | *C5* |
|---|---|---|---|---|---|
| *v* | -2.63946e-5 | 1.29911e-8 | 6.74940e-9 | -1.91909e-5 | 1.95486e-8 |
| *b* | 1.54917e-6 | 2.45532e-8 | 4.22922e-9 | -1.36861e-5 | 1.61345e-8 |
| *u* | -2.07989e-5 | 2.90123e-8 | 1.43053e-10 | -2.22924e-5 | 1.36663e-10 |

Figure 2 show contour plots of the derived LSS for the *u* (black), *b* (blue) and *v* (red) filters in raw image coordinates. The minimum and maximum correction factors for each filter over the 2048 by 2048 raw image are listed in Table 1. The *v* contour is similar to the coarse LSS sensitivity map shown in Figure 8 of Poole et al. (2007, MNRAS, 383, 627) which was created using the same GD 50 data All three filters are similar in having increased sensitivity toward the lower left-hand corner of the raw image. However, the contours for the three filters are distinct and not interchangeable. In particular the LSS correction for the *b* filter is smaller than for either the *u* or *v* filter.

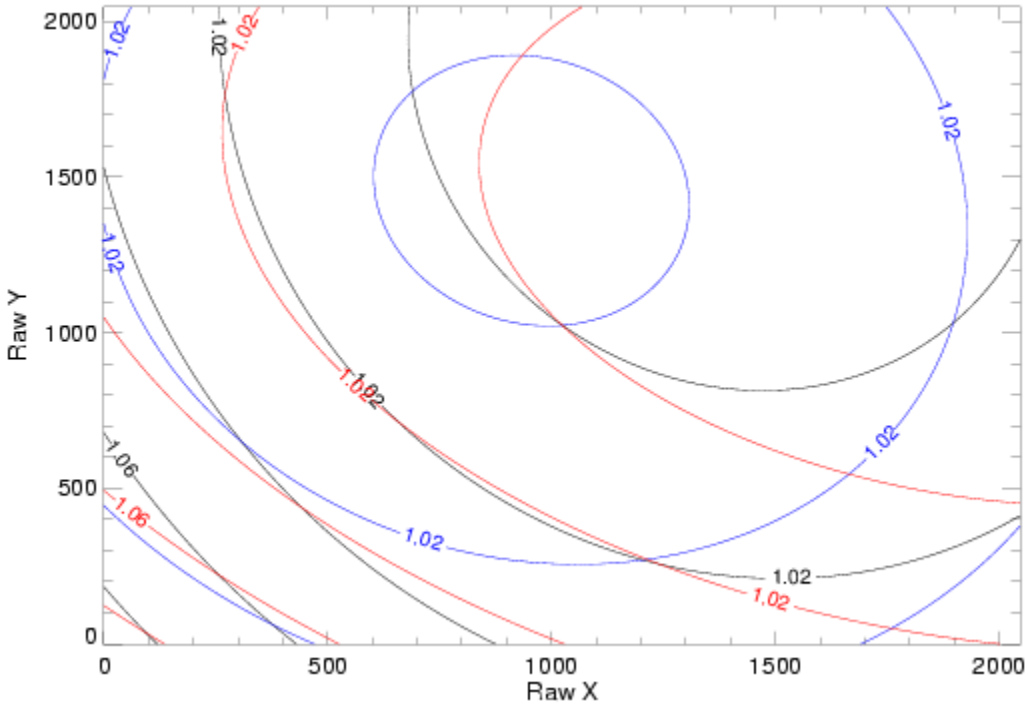


Figure 1. LSS contours for the *u* (black), *b* (blue) and *v* (red) filters

C. Verification:

The use of the LSS should improve the comparison between UVOT and external photometry in a standard star field. Figure 3 compares UVOT photometry of the PG 1633+099B field with and without an LSS correction with that of Stetson (2000, PASP, 112, 925). (This field was previously used by Poole et al. to study the effects of an aperture correction on UVOT photometry.) The color term correction given by Poole et al. was used to convert UVOT *v* to Johnson V. The use of the LSS is seen to significantly reduce the scatter between UVOT and Stetson photometry. For stars with V < 16.5 the scatter is reduced from 0.033 mag to 0.024 mag.

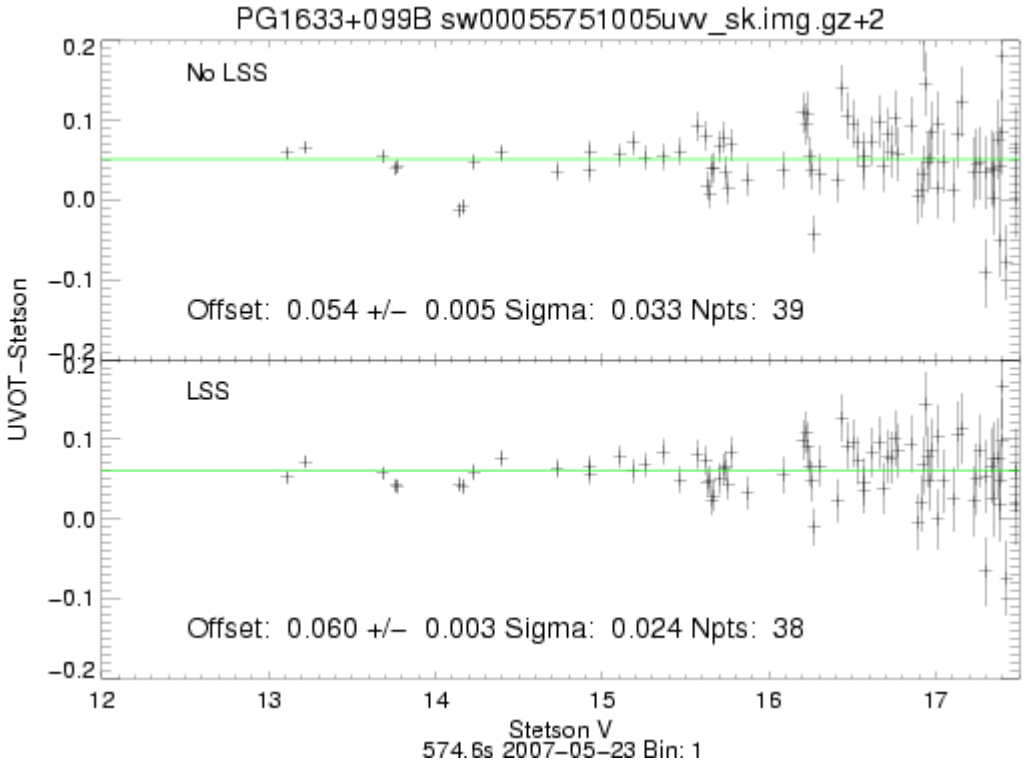


Figure 2: UVOT *v* photometry with (below) and without (top) an LSS correction compared to V photometry of Peter Stetson

More than 30 plots similar to Figure 3 have been created by comparing UVOT v data to photometry from Stetson or the Sloan "Stripe 82" field (Ivezic et al. 2007, AJ, 134, 973). With a couple of exceptions, these plots all show a decrease in the photometric scatter with use of a LSS.

A similar test for the *b* filter is not as clear-cut because the LSS correction is smaller in *b* than in *v*, and because the scatter between *b* and Johnson B is larger than between *v* and Johnson V. (Note that the color term formulae given by Poole et al. (2007) was not used to convert UVOT *b* to Johnson B because it appears to increase the scatter. ) However, there is an overall trend showing improved *b* photometry with use of the LSS, as illustrated in Figure 4 for the same PG 1633+099 B field.

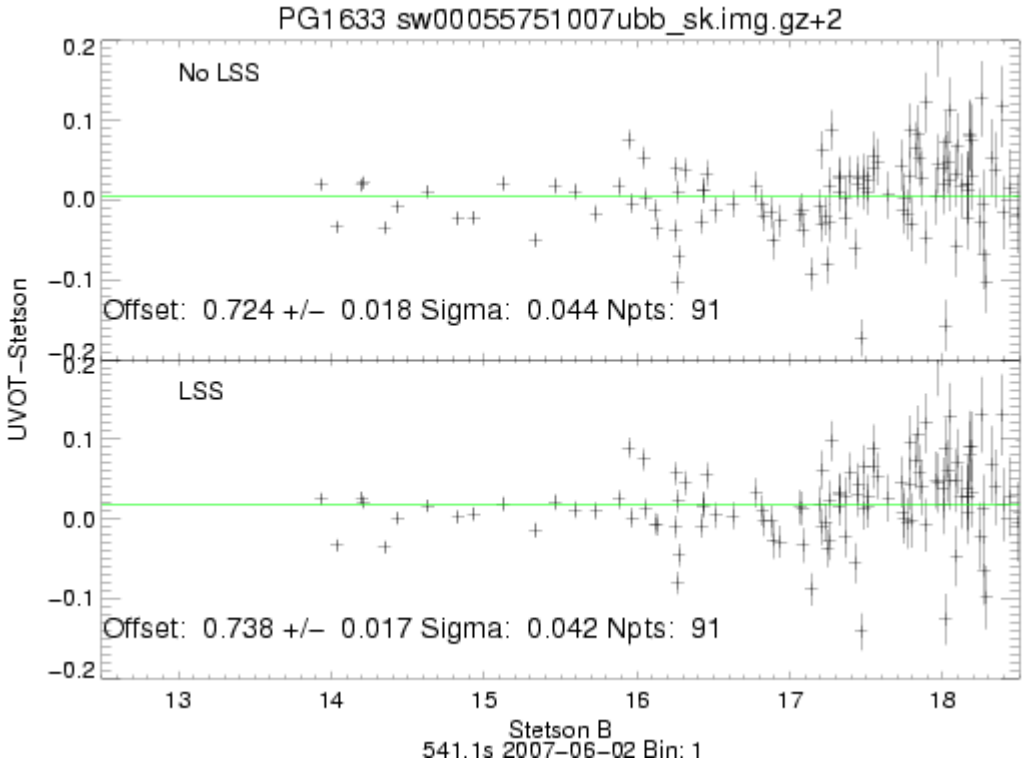


Figure 4: UVOT *b* photometry with (bottom) and without (top) an LSS correction compared to Johnson B photometry from Stetson.

A similar comparison of the UVOT *u* filter with standard star fields is not possible because of the large difference between the UVOT *u* and Johnson U filters, and because of the limited availability and accuracy of Johnson U data. However, there are 122 *u* filter pointings of the Extended Chandra Deep Field (ECDF), taken over a 6 month interval. Figure 5 and 6 show the photometry of two stars which appreciably change their raw detector position as the roll angle changes. (Star 4 is located at 03 31 58.72 -27 46 35.1 with B ≈ 15.4 and star 5 is located at 03 32 50.45 -27 48 33.0 with B ≈ 14.4) The use of the LSS clearly improves the *u* photometry for these two stars.

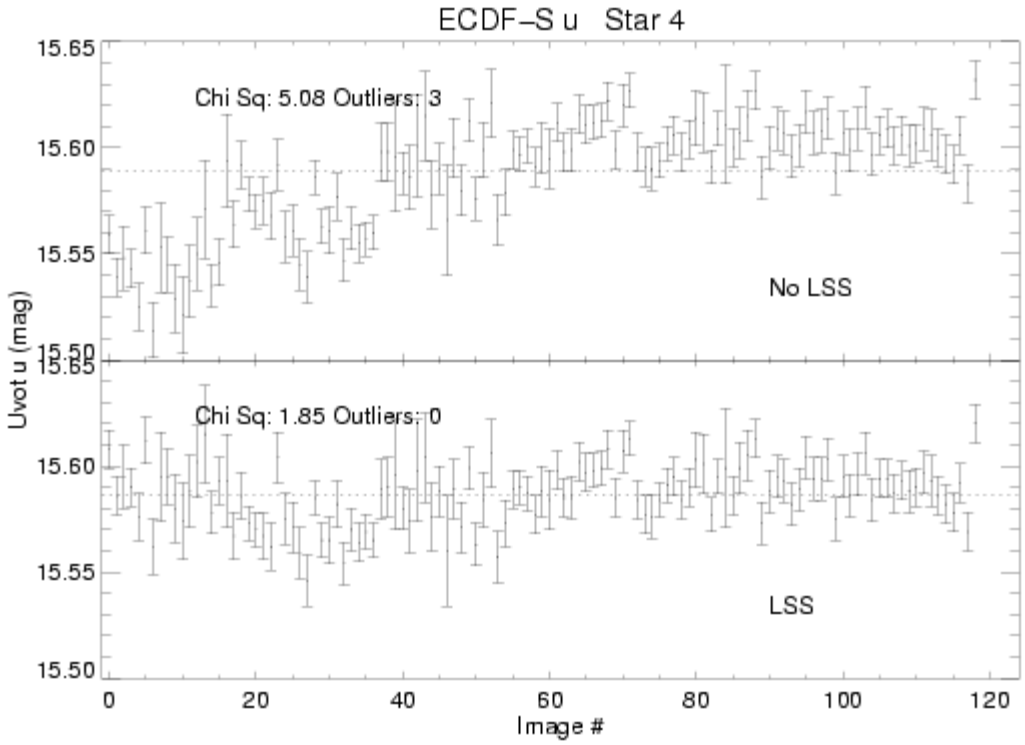


Figure 4: UVOT *u* photometry of a star in the ECDF field with (bottom) and without (top) an LSS correction.

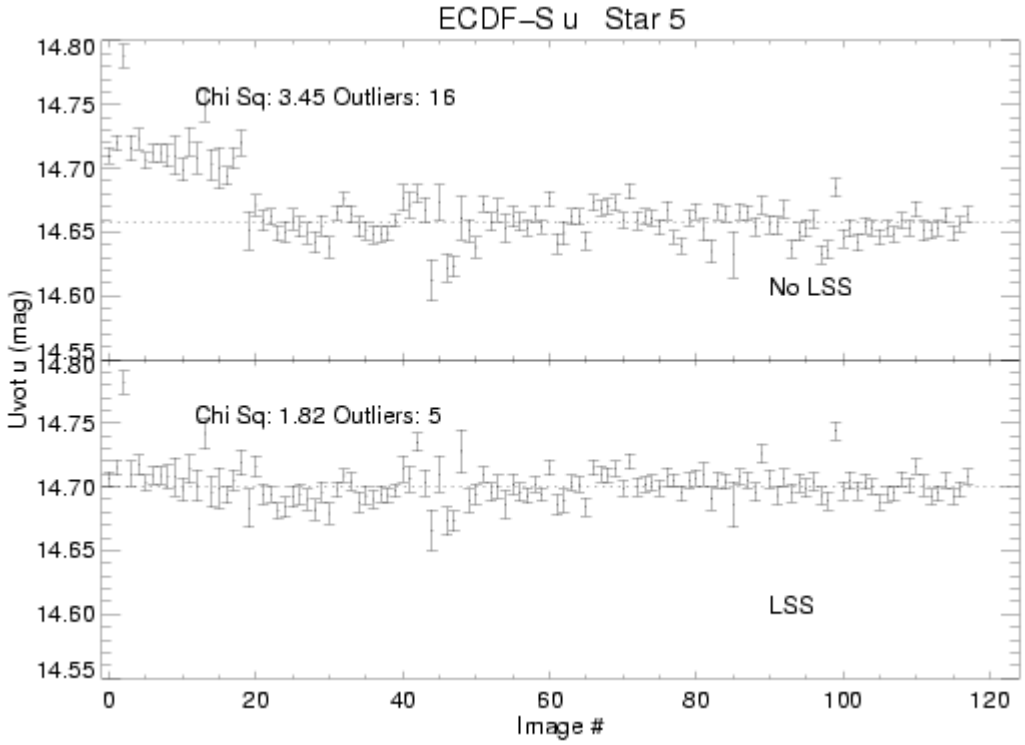


Figure 5: UVOT *u* photometry of a star in the ECDF field with (bottom) and without (top) an LSS correction.